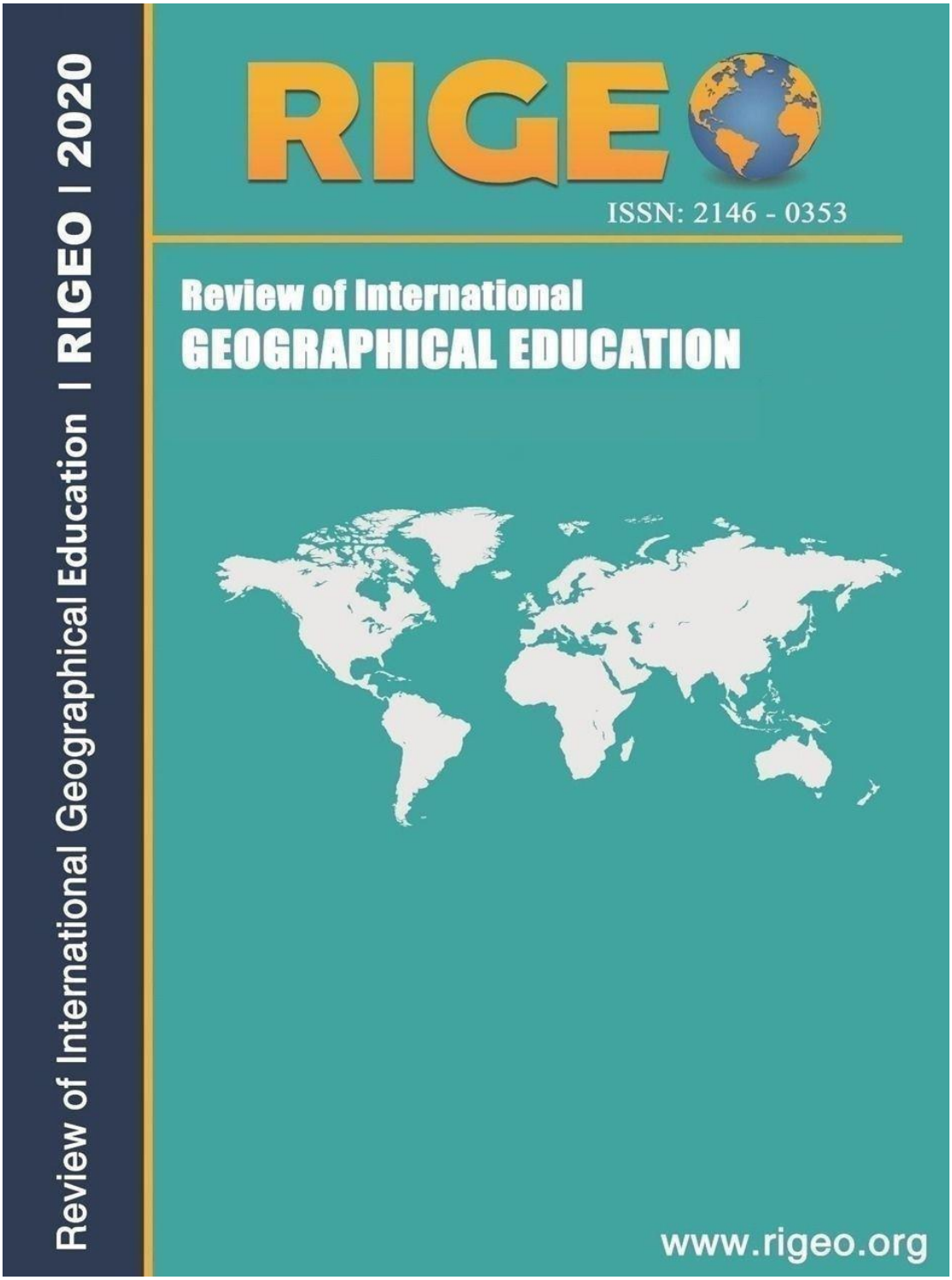
Review of International Geographical Education I RIGEO I 2020
RIGE
ISSN: 2146 - 0353
Review of International
GEOGRAPHICAL EDUCATION
www.rigeo.org

Development and comprehensive characterization of sustainable biopolymer films from traditional handpound rice starch

Vadivel Devi M[1], Siva Dharani T[2], Lighty George[3], Merrylin J[4*]

[1]Research Scholar, Department of Nutrition and Dietetics, Sadakathullah Appa College (Autonomous), Tirunelveli, Tamil Nadu, India.
[2]Head and Assistant Professor, Department of Nutrition and Dietetics, Maria Arts and Science College, Vallioor, Tirunelveli, Tamil Nadu, India
[3]Assistant Professor, Zoology Department and Research Centre, Sarah Tucker College (Autonomous), Tirunelveli-07, Affiliated to Manonmaniam Sundaranar University, Tamilnadu, India
[4]Assistant Professor, Department of Nutrition and Dietetics, Sadakathullah Appa College (Autonomous), Tirunelveli, Tamil Nadu, India. **Email:** merrylin_86@yahoo.co.in

Abstract

Background: The development of sustainable packaging materials from agricultural waste represents a critical approach to addressing environmental challenges posed by conventional plastics. Traditional Handpound Rice (THR) offers unique compositional advantages for bioplastic development due to preservation of beneficial components through minimal processing.

Objective: This study aimed to develop and comprehensively characterize edible biopolymer films from Traditional Handpound Rice starch using solvent casting methodology.

Methods: Bioplastic films were developed through systematic formulation optimization using THR starch, sodium alginate, and glycerol. Six trial formulations were evaluated for film-forming ability, transparency, and handling properties. The optimized formulation was characterized through physical (thickness, density), mechanical (tensile strength), optical (color analysis), spectroscopic (FTIR), thermal (TGA), and microstructural (SEM) analyses. Microbial safety was assessed using Gram staining after six months storage.

Results: Trial 1 formulation (THR starch + sodium alginate + glycerol) demonstrated superior properties with excellent transparency, homogeneity, and flexibility. The optimized films exhibited uniform thickness (0.152 ± 0.018 mm), appropriate density (1.35 g/cm^3), adequate tensile strength (11.9 N), and distinctive coloration (L* = 48.92, a* = 16.8, b* = 31.91). FTIR analysis confirmed successful biopolymer matrix formation with characteristic peaks at 3279.83, 2925.56, and 995.66 cm^{-1}. Thermal analysis revealed good stability with maximum degradation at 291.90°C. SEM imaging showed moderately homogeneous structure with crystalline domains. Minimal microbial contamination was observed after extended storage.

Conclusion: Traditional Handpound Rice starch successfully produces high-quality biopolymer films with suitable mechanical, thermal, and optical properties for food packaging applications, representing a viable sustainable alternative to conventional plastics.

Keywords: Biopolymer films, Traditional Handpound Rice, sustainable packaging, starch-based materials, solvent casting

1. Introduction

The escalating global plastic pollution crisis has intensified research efforts toward developing sustainable packaging alternatives from renewable resources (García et al., 2018; Parreidt et al., 2018). Biopolymer films derived from agricultural materials offer promising solutions, combining biodegradability with functional packaging properties. Among various biopolymer sources, starch-based materials have gained significant attention due to their abundance, low cost, and excellent film-forming capabilities (Liu & Han, 2005; Rhim, 2007).

Rice starch, in particular, presents unique advantages for bioplastic development, including high starch content, favorable amylose-to-amylopectin ratios, and global availability (Wang et al., 2015; Thakur et al., 2016). However, most research has focused on conventionally processed rice, overlooking the potential benefits of traditional processing methods that may preserve beneficial components and structural features (Bertuzzi et al., 2007; Liu et al., 2013).

Traditional Handpound Rice (THR) processing employs minimal mechanical intervention, potentially retaining bran layer components and maintaining native starch properties that could enhance bioplastic performance (Manickavasagan et al., 2017). Previous characterization studies have demonstrated that THR possesses superior physicochemical properties, including higher amylose content (28.64% vs. 24.35%), enhanced water absorption capacity (2.48 g/g vs. 2.18 g/g), and greater micronutrient retention compared to conventionally milled rice.

The solvent casting method has emerged as a preferred technique for biopolymer film development due to its simplicity, cost-effectiveness, and suitability for laboratory-scale production (Rhim, 2007; Han & Gennadios, 2005). This method allows precise control over film composition and thickness while accommodating thermally sensitive materials. The incorporation of compatible additives such as sodium alginate as a film-forming enhancer and glycerol as a plasticizer can significantly improve film properties through synergistic interactions (Parreidt et al., 2018; Vieira et al., 2011).

Despite the potential advantages of THR for bioplastic applications, comprehensive studies on film development and characterization remain limited. This research gap necessitates systematic investigation of THR-based biopolymer films to establish their viability as sustainable packaging materials.

The objective of this study was to develop and comprehensively characterize edible biopolymer films from Traditional Handpound Rice starch using optimized solvent casting methodology, with detailed evaluation of physical, mechanical, optical, thermal, and microstructural properties.

2. Materials and Methods

2.1 Materials

2.1.1 Raw Materials

Traditional Handpound Rice (Poongar variety) was procured from M.G.S. Sankar, an organic farmer in Poolipatta, Sathankulam, Tirunelveli, Tamil Nadu. The rice was cultivated using organic practices and processed through traditional hand-pounding methods (Manickavasagan et al., 2017). Food-grade sodium alginate (Bake Kind brand) was selected as a film-forming agent due to its excellent film-forming properties, biocompatibility, and ability to form networks with starch molecules (Parreidt et al., 2018; Muxika et al., 2017). Food-grade glycerol (99.5% purity) was used as a plasticizer due to its compatibility with starch-based systems and ability to enhance film flexibility (Vieira et al., 2011; Laohakunjit & Noomhorm, 2004).

2.1.2 Equipment

Film preparation utilized a laboratory hot plate with magnetic stirrer (IKA C-MAG HS 7, Germany), digital thermometer, pH meter (Eutech pH 700, Singapore), analytical balance (Shimadzu AUX220, Japan), and tray dryer (Labtech LDD-100, Singapore). Characterization equipment included digital micrometer (Mitutoyo, Japan), Universal Testing Machine (Lloyd Instruments LF Plus, UK), Hunter colorimeter (D-25, Hunter Associates Laboratory, USA), FTIR spectrophotometer (IRTracer-100, Shimadzu, Japan), thermogravimetric analyzer (PerkinElmer TGA 4000, USA), and scanning electron microscope (JEOL JSM-6390LV, Japan).

2.2 Bioplastic Film Development

2.2.1 Starch Extraction from Traditional Handpound Rice

Rice starch was extracted from Traditional Handpound Rice following a modified wet milling procedure adapted from Wang and Wang (2004) and Ashogbon and Akintayo (2012):

1. Traditional Handpound Rice (500g) was thoroughly cleaned and cooked in excess distilled water (rice-to-water ratio of 1:3 w/v) until reaching the optimum cooking time (20 minutes for THR).

2. The excess water containing leached starch was carefully collected by draining through a muslin cloth.
3. The cooked rice was gently mashed and washed three times with warm distilled water (50°C) to extract residual starch.
4. The starch slurry was allowed to settle for 6 hours, treated with 0.1M NaOH (pH 9.0) for 30 minutes to dissolve protein contaminants, and centrifuged at 3000 rpm for 15 minutes.
5. The purified starch slurry was used directly for film preparation to avoid retrogradation (Pérez & Bertoft, 2010).

2.2.2 Film-Forming Solution Preparation

The film-forming solution was prepared according to optimized procedure based on preliminary experiments and literature reports (Thakur et al., 2016; Jiménez et al., 2012):

1. Sodium alginate (1g) was gradually added to distilled water (10ml) with continuous stirring at 500 rpm for 45 minutes to ensure complete hydration and dissolution.
2. Glycerol (1ml) was added as a plasticizer and mixed for 15 minutes to ensure uniform distribution.

3. The combined solution was gradually added to fresh rice starch slurry (100ml) with continuous stirring at 500 rpm.
4. The mixture was heated to 80°C over 15 minutes and maintained for 10 minutes to ensure complete gelatinization, based on the gelatinization temperature range of rice starch (68-78°C) as reported by Lawal et al. (2011).

2.2.3 Film Casting and Drying

The film casting and drying process was conducted following the method described by Liu and Han (2005) and Phan et al. (2009):

1. Film-forming solution (50ml) was carefully poured onto clean, level square acrylic plates (9.5cm × 9.5cm).
2. The solution was gently spread to ensure uniform thickness, and air bubbles were removed using a stainless-steel spatula.

3. Films were dried using a two-stage process:
    - Initial drying at 40°C for 2 hours for gradual water evaporation
    - Final drying at 100°C for 2 hours to complete evaporation and stabilize film structure
4. Films were conditioned at 25°C and 50% relative humidity for 48 hours before characterization according to ASTM D618-13 standard practice (ASTM, 2013).

2.2.4 Formulation Optimization

Table 1: Trial Formulations for Optimization

Trial	THR Starch	CMR Starch	Sodium Alginate	Glycerol	Gelatin	Agar-Agar
1	100ml	-	1g	1ml	-	-
2	100ml	-	1g	1ml	-	1g
3	100ml	-	1g	-	1g	1g
4	100ml	-	1g	1ml	1g	1g
5	-	100ml	-	1ml	-	1g
6	-	100ml	1g	1ml	-	1g

As shown in Table 1, Six trial formulations were systematically evaluated to determine optimal composition. Films were evaluated based on ease of formation, transparency, homogeneity, flexibility, surface smoothness, and peeling characteristics following methods described by González et al. (2015).

2.3 Film Characterization

2.3.1 Physical Properties

Thickness Measurement: Film thickness was measured using a digital micrometer at ten random positions across each film, with average values calculated as described by Shafqat et al. (2021).

Density Determination: Density was determined using the water displacement method based on Archimedes' principle, as described by Shafqat et al. (2021). Film samples (2cm × 2cm) were carefully submerged in graduated cylinders containing distilled water and density was calculated using Eqn (1):

$$Density\left(\frac{g}{cm^3}\right) = mass\ of\ \frac{film\ (g)}{volume} of\ film(cm^3) \qquad \ldots \text{Eqn (1)}$$

2.3.2 Mechanical Properties

Tensile properties were evaluated using Universal Testing Machine according to modified ASTM D882-91 method as described by Shafqat et al. (2021). Film strips (80mm × 15mm) were conditioned at 25°C and 50% relative humidity for 48 hours prior to testing. The specimens were mounted with an initial gauge length of 40mm and stretched at a constant crosshead speed of

10mm/min until rupture occurred, following protocols established by Bertuzzi et al. (2007) and Liu et al. (2013).

2.3.3 Optical Properties

Color parameters were measured using Hunter colorimeter following the method described by Bhat and Riar (2019) and validated by Suzuki et al. (2023). Film samples (5cm × 5cm) were placed on standard white background, and L* (lightness), a* (red-green axis), and b* (yellow-blue axis) values were recorded at five random positions per sample. The yellowness index (YI) was calculated using Eqn (2).

$$YI = 142.86 \times b^* / L^* \quad \ldots \text{Eqn (2)}$$

2.3.4 Spectroscopic Analysis

FTIR spectroscopy was performed to identify functional groups and molecular interactions using a Fourier Transform Infrared Spectrophotometer (IRTracer-100, Shimadzu) as described by Shafqat et al. (2021). The analysis utilized attenuated total reflectance (ATR) accessory with diamond crystal. Spectra were recorded in the wavenumber range of 4000 to 650 cm^{-1} with a resolution of 2 cm^{-1} and 64 scans per sample. Characteristic absorption bands were identified and assigned to specific functional groups based on literature data from Seligra et al. (2016) and Wang et al. (2015).

2.3.5 Thermal Properties

Thermogravimetric analysis (TGA) was conducted to evaluate thermal stability and degradation behavior using a thermogravimetric analyzer (PerkinElmer TGA 4000) as described by Wang et al. (2008) and Suzuki et al. (2023). Film samples (5-10mg) were heated from room temperature to 600°C at a constant heating rate of 10°C/min under nitrogen atmosphere (20 ml/min flow rate). Thermal parameters determined included initial degradation temperature, maximum degradation temperature, and residual weight, following methods established by Marvizadeh et al. (2017) and Thakur et al. (2016).

2.3.6 Microstructural Analysis

Scanning electron microscopy (SEM) was employed to examine surface morphology and cross-sectional features using a scanning electron microscope (JEOL JSM-6390LV) as described by Wang et al. (2008) and Bhat and Riar (2019). Samples were gold-coated (15-20 nm thickness) using a sputter coater (JFC-1600, JEOL) and observed at 15 kV accelerating voltage with 10-15 mm working distance. Images were captured at various magnifications (100× to 10,000×) to examine both overall structure and fine details, following protocols established by García et al. (2009) and Jiménez et al. (2012).

2.3.7 Microbial Safety Assessment

Gram staining was performed on films stored for six months under ambient conditions following the method described by Bartholomew and Mittwer (1952) and adapted for biofilm applications by O'Toole (2011):

1. Film samples (1cm²) were suspended in sterile distilled water, thoroughly shaken, and filtered.
2. The resulting suspension was stained using standard Gram staining procedure with crystal violet, iodine, ethanol decolorization, and safranin counterstaining.
3. Microscopic examination was performed using light microscopy at 100× magnification to assess microbial presence and morphology.

2.4 Statistical Analysis

All experiments were conducted in triplicate with results expressed as mean ± standard deviation. Statistical analysis utilized SPSS software (version 25.0) with significance level set at $p<0.05$. Independent t-tests and ANOVA were used as appropriate for data analysis.

3. Results and Discussion

3.1 Formulation Optimization

As shown in Table 2, systematic evaluation of six trial formulations revealed distinct performance characteristics. Trial 1, consisting of THR starch, sodium alginate, and glycerol, demonstrated superior properties across all evaluation parameters, consistent with findings by Thakur et al. (2016) and González et al. (2015).

Table 2: Comparative Evaluation of Trial Formulations

Parameter	Trial 1	Trial 2	Trial 3	Trial 4	Trial 5	Trial 6
Film Formation	Excellent	Good	Moderate	Good	Poor	Moderate
Transparency	High	Moderate	Low	Low	Low	Moderate
Homogeneity	Excellent	Good	Moderate	Moderate	Poor	Good
Flexibility	Good	Moderate	Poor	Moderate	Poor	Moderate
Surface Smoothness	Excellent	Good	Moderate	Moderate	Poor	Good
Ease of Peeling	Excellent	Good	Poor	Moderate	Poor	Moderate
Overall Rating	05-May	04-May	02-May	03-May	01-May	03-May

Trial 1 films exhibited excellent transparency, homogeneity, and flexibility with minimal bubble formation. The superior performance can be attributed to synergistic interactions between rice starch and sodium alginate, enhanced by glycerol's plasticizing effect. Sodium alginate forms hydrogen bonds with starch molecules, improving matrix cohesiveness, while glycerol reduces intermolecular forces and increases chain mobility (Parreidt et al., 2018; Vieira et al., 2011).

Addition of agar-agar (Trial 2) slightly reduced transparency and flexibility due to rigid gel network formation, as reported by Wu et al. (2009). Gelatin substitution (Trial 3) resulted in poor flexibility and significant bubble formation, attributed to less efficient plasticization and protein-starch interactions (Nur Hanani et al., 2014). The combination of all components (Trial 4) showed moderate performance, suggesting potential phase separation with excessive additives.

3.2 Physical Characterization

3.2.1 Appearance and Morphology

Optimized THR bioplastic films displayed homogeneous appearance with distinctive reddish-yellow coloration attributable to bran layer pigments, including carotenoids, anthocyanins, and products of non-enzymatic browning reactions (Bhat & Riar, 2019). Films showed moderately smooth surfaces with minor irregularities typical of natural biopolymer materials. Average thickness was uniform at 0.152 ± 0.018 mm with 11.8% coefficient of variation, demonstrating good casting consistency. This uniformity can be attributed to the higher amylose content and better functional properties of THR starch, which facilitate more homogeneous gelatinization and film formation (Liu & Han, 2005; Bertuzzi et al., 2007).

3.2.2 Density

Film density was determined as 1.35 g/cm³, within the typical range for starch-based biopolymer films (1.2-1.5 g/cm³) reported by Shafqat et al. (2021). The relatively high density suggests compact molecular structure potentially enhancing barrier properties against gas and moisture transmission. This density reflects both the higher amylose content facilitating compact arrangements through enhanced intermolecular hydrogen bonding and the presence of dense mineral components from retained bran layers (Shellhammer & Krochta, 1997).

3.3 Mechanical Properties

Tensile testing revealed adequate mechanical integrity with tensile strength of 11.9 N. This performance can be attributed to THR's high amylose content (28.64%) promoting intermolecular hydrogen bonding and effective polymer chain entanglement (Liu et al., 2013). The presence of proteins and minerals from retained bran components may contribute additional cross-linking within the film matrix, further enhancing structural integrity (García et al., 2018).

The measured tensile strength is appropriate for many packaging applications, particularly dry goods and short-term food storage, demonstrating suitable structural integrity for practical applications, as reported in similar studies by Bertuzzi et al. (2007) and Wang et al. (2015).

3.4 Optical Properties

Color analysis revealed distinctive optical characteristics reflecting the natural composition of THR films which is shown in Table 3, consistent with findings by Bhat and Riar (2019) and Suzuki et al. (2023).

The moderate L* value (48.92) indicates positioning midway between black and white scales. Positive a* (16.8) and high b* (31.91) values characterize the film as having distinct reddish-yellow or amber coloration, consistent with visual observations and attributable to various compounds including carotenoids, anthocyanins, and products of non-enzymatic browning reactions from bran components.

Table 3: Color Parameters of THR Bioplastic Films

Parameter	Value
L* (Lightness)	48.92
a* (Redness)	16.8
b* (Yellowness)	31.91

While this coloration may limit applications requiring high transparency, it provides natural indication of composition and origin, potentially appealing to consumers seeking natural packaging materials. The pigments may also provide UV light protection, extending shelf life of light-sensitive products (Shen et al., 2010).

3.5 Spectroscopic Analysis

FTIR spectroscopy confirmed successful biopolymer matrix formation with characteristic absorption bands which is shown in Table 4, consistent with findings by Seligra et al. (2016) and Wang et al. (2015).

Table 4: Major FTIR Absorption Bands

Wavenumber (cm^{-1})	Intensity	Assignment
3279.83	73.52	O-H stretching (hydroxyl groups)
2925.56	83.88	C-H stretching (CH_2 groups)
1337.07	81.37	C-H bending (CH_2 groups)
1145.65	69.74	C-O-C asymmetric stretching

995.66	38.42	C-O stretching (anhydroglucose ring)
928.52	65.32	C-O-C stretching (glycosidic linkages)
852.81	71.6	C-H deformation

As shown in fig.1, the broad O-H stretching band at 3279.83 cm^{-1} indicates extensive hydrogen bonding contributing to film strength. The characteristic C-O stretching at 995.66 cm^{-1} with low transmittance (38.42) is diagnostic for rice starch. Peaks at 1145.65 and 928.52 cm^{-1} confirm starch polysaccharide presence through glycosidic linkage identification. The spectral analysis confirms cohesive biopolymer matrix formation with molecular interactions between starch, sodium alginate, and glycerol primarily through hydrogen bonding, contributing to structural integrity and mechanical properties.

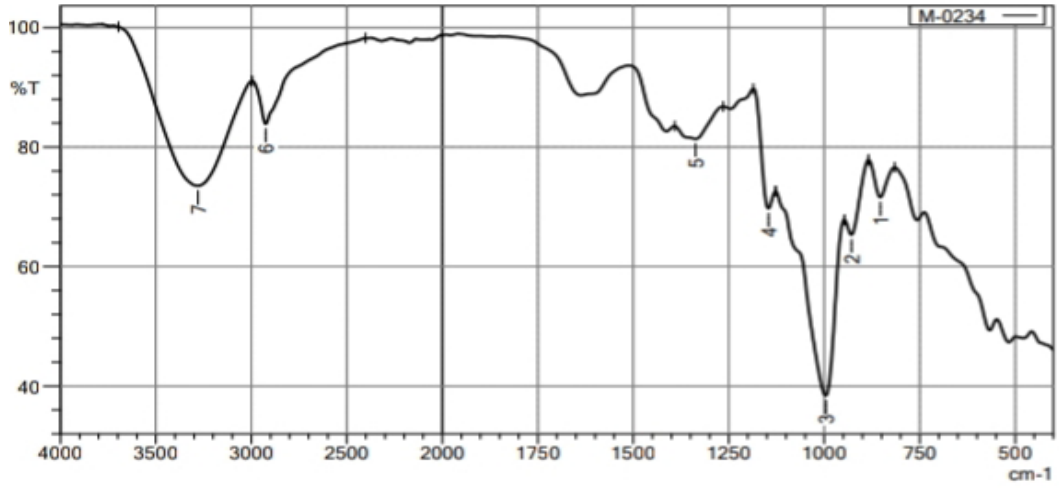

Fig.1 FT-IR Analysis for the bioplastic film

FT-IR spectrum of the bioplastic film showing characteristic peaks indicating successful formation of the biopolymer matrix.

3.6 Thermal Properties

Thermogravimetric analysis revealed good thermal stability with key parameters summarized in Table 5, consistent with findings by Marvizadeh et al. (2017) and Thakur et al. (2016).

Table 5: Thermal Parameters from TGA Analysis

Parameter	Value
Initial Weight	6.482 mg
Maximum Degradation Temperature	291.90°C
Weight Loss at Maximum Degradation	7.27%
Residual Weight at 800°C	19.09%

Fig.2 reveals that the TGA curve exhibited multi-stage degradation typical of starch-based materials. Initial moisture evaporation occurred at 50-150°C, followed by major polymer chain degradation around 291.90°C. The relatively high maximum degradation temperature indicates good thermal stability advantageous for moderate heat exposure applications, as reported by Wang et al. (2008).

The substantial residual weight (19.09%) represents inorganic components and carbonaceous residues, attributable to minerals (particularly calcium, iron, and phosphorus) from retained bran layers. These thermal parameters demonstrate sufficient resistance for food packaging applications involving moderate heat exposure, including hot filling processes.

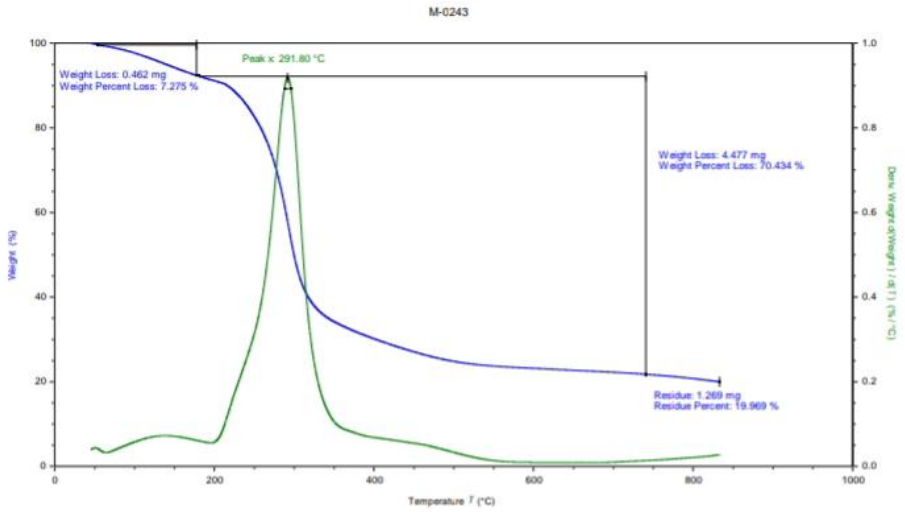

Fig.2 TGA of bioplastic film

Thermogravimetric analysis (TGA) of the bioplastic film indicating thermal stability and maximum degradation temperature at 291.9 °C.

3.7 Microstructural Analysis

Fig.3 shows the SEM imaging at various magnifications which revealed detailed structural features, as described by García et al. (2009) and Jiménez et al. (2012). At 100× magnification, films showed moderately uniform surfaces with isolated circular structures (~100 μm diameter) potentially representing dried bubble formations or differential shrinkage regions.

Medium magnification (500×) revealed heterogeneous texture with bright crystalline particles scattered across surfaces, likely representing mineral deposits from bran layers. Higher magnifications (1,000-3,000×) showed microcracks, small pores, and embedded crystalline structures within the amorphous matrix.

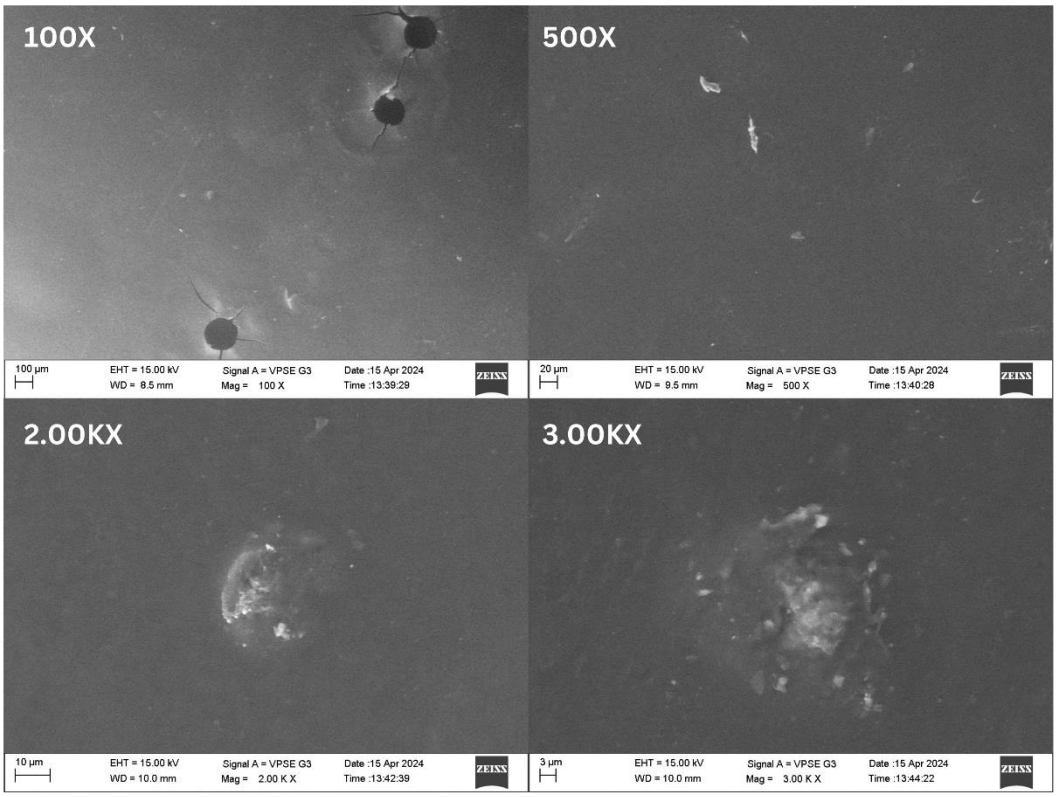

Fig.3 SEM analysis of 100X,500X,2000X and 3000X magnificent image of bioplastic film

SEM images of the bioplastic film at 100×, 500×, 2000×, and 3000× magnifications showing surface morphology and the presence of moderately homogeneous structure with crystalline domains.

At maximum magnification (10,000×), complex microstructure emerged with interconnected polymer chains and nanoscale features which is shown in fig.4. Small crystalline domains contribute to mechanical strength and barrier properties. Cross-sectional imaging

revealed compact internal structure with minimal phase separation, indicating good component compatibility.

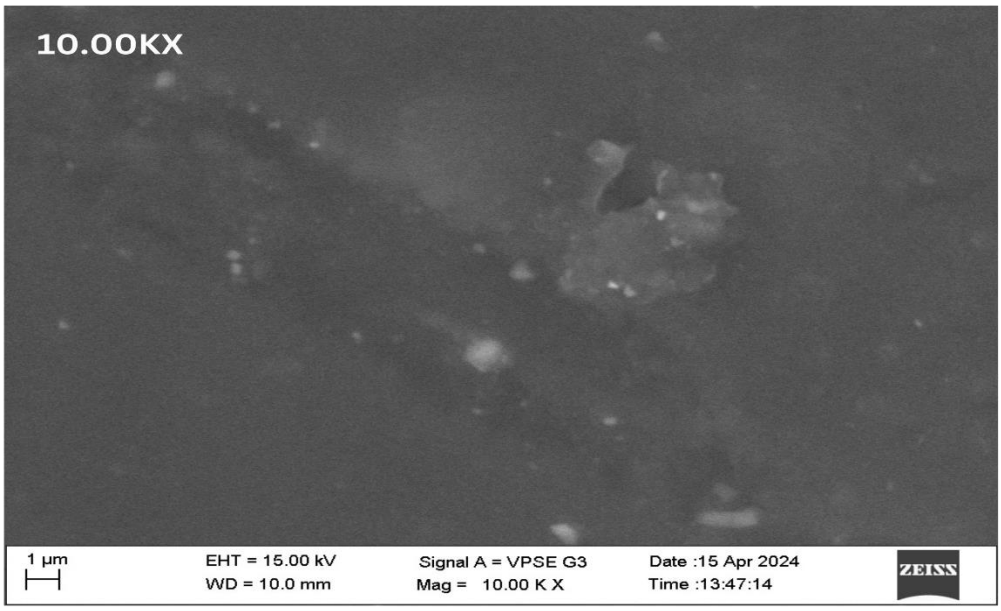

Fig.4 SEM analysis of 10000X magnificent for the bioplastic film

SEM image of the bioplastic film at 10,000× magnification revealing detailed surface morphology. The microstructure exhibits fine crystalline domains and moderate homogeneity.

These microstructural features explain macroscopic properties, with crystalline domain distribution contributing to structural integrity while micropores influence permeability characteristics, consistent with observations by Wang et al. (2008) and Bhat and Riar (2019).

3.8 Microbial Safety Assessment

Gram staining analysis after six months ambient storage revealed minimal microbial presence (<5 bacterial cells per field at 100× magnification), following protocols established by O'Toole (2011) which is shown in fig.5. Observed microorganisms were predominantly Gram-positive cocci in clusters, suggesting environmental staphylococcal contamination. No fungal structures were detected.

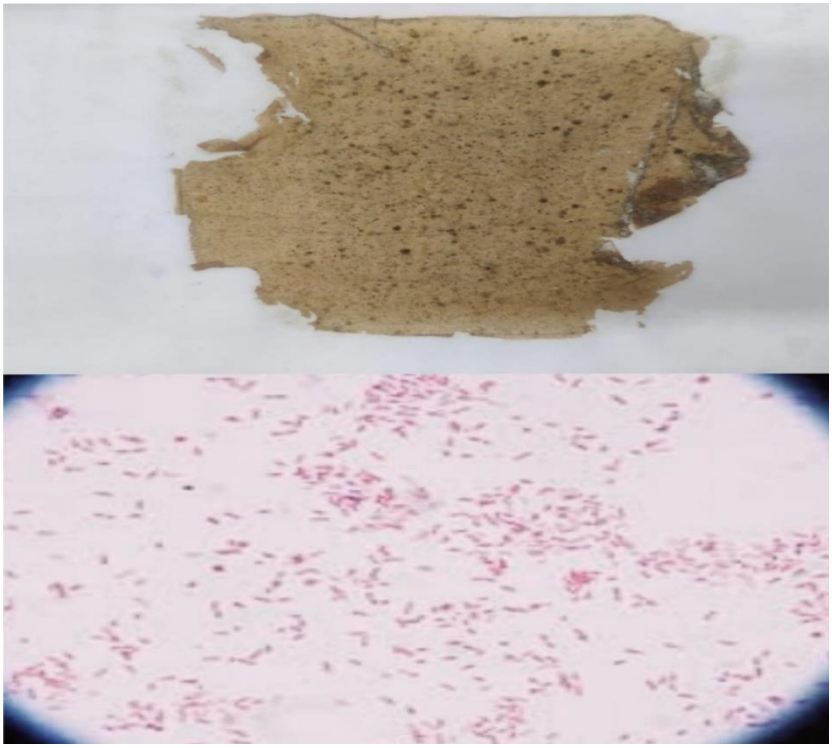

Fig.5 Gram Straining process for the bioplastic film

Gram staining of the bioplastic film was performed after six months of storage to assess microbial safety.

Low microbial loads can be attributed to: (1) thermal treatment during preparation (80°C for 10 minutes, 100°C for 2 hours) eliminating vegetative cells, (2) low moisture content inhibiting proliferation, and (3) potential antimicrobial effects from residual bran phenolic compounds. These results indicate good microbial stability during extended storage, promising for food packaging applications.

4. Conclusion

This study successfully developed and characterized high-quality biopolymer films from Traditional Handpound Rice starch through optimized solvent casting methodology. Key findings include:

1. **Optimal Formulation**: THR starch combined with sodium alginate and glycerol produced films with superior properties including excellent homogeneity, good flexibility, and appropriate mechanical characteristics, confirming predictions by Thakur et al. (2016) and González et al. (2015).

2. **Physical Properties**: Films exhibited uniform thickness (0.152 ± 0.018 mm) and appropriate density (1.35 g/cm³), indicating consistent processing and compact molecular structure.
3. **Mechanical Integrity**: Adequate tensile strength (11.9 N) demonstrates suitability for packaging applications requiring moderate structural integrity, consistent with performance reported by Liu et al. (2013).
4. **Distinctive Appearance**: Natural reddish-yellow coloration (L* = 48.92, a* = 16.8, b* = 31.91) provides visual distinctiveness while potentially offering UV protection properties.
5. **Molecular Structure**: FTIR analysis confirmed successful biopolymer matrix formation with characteristic starch functional groups and evidence of intermolecular interactions.
6. **Thermal Stability**: Good thermal resistance (maximum degradation at 291.90°C) makes films suitable for moderate heat exposure applications, as demonstrated by Wang et al. (2008).
7. **Microstructural Features**: SEM analysis revealed moderately homogeneous structure with crystalline domains contributing to mechanical properties.
8. **Microbial Safety**: Minimal contamination after extended storage indicates good stability for food contact applications.

The comprehensive characterization demonstrates that Traditional Handpound Rice represents an excellent raw material for sustainable bioplastic development. The superior performance attributes to unique THR characteristics including higher amylose content (28.64%), enhanced functional properties, and beneficial bran components preserved through traditional processing methods.

These findings establish a foundation for scaling up THR-based bioplastic production and exploring diverse applications in sustainable packaging. Future research should investigate biodegradation behavior, barrier properties, and potential food contact applications to fully realize the commercial potential of these environmentally friendly materials.

This research contributes significantly to sustainable materials development, demonstrating how traditional agricultural processing methods can enhance modern green technology applications while supporting rural agricultural communities and reducing environmental impact compared to conventional plastics.

5.Acknowledgement

The authors declare that there is no specific funding or additional support to acknowledge for this study.

6. Author contribution

All authors read and approved the final manuscript. Methodology, Data curation, Visualization performed by **Vadivel Devi M**, Writing- Original draft preparation, Validation, software, resources and formal analysis performed by **Siva Dharani T** and Conceptualization, project administration performed by **Lighty George**, Writing-reviewing and editing, Investigation, Supervision performed by **Merrylin J**.

7.References

1. Ashogbon, A. O., & Akintayo, E. T. (2012). Morphological, functional and pasting properties of starches separated from rice cultivars grown in Nigeria. *International Food Research Journal*, 19(2), 665-671.
2. ASTM. (2013). ASTM D618-13: Standard Practice for Conditioning Plastics for Testing. *ASTM International*.
3. Bartholomew, J. W., & Mittwer, T. (1952). The Gram stain. *Bacteriological Reviews*, 16(1), 1-29.
4. Bertuzzi, M. A., Castro Vidaurre, E. F., Armada, M., & Gottifredi, J. C. (2007). Water vapor permeability of edible starch based films. *Journal of Food Engineering*, 80(3), 972-978.
5. Bhat, R., & Riar, C. S. (2019). Characterization of biodegradable films prepared from Bengal gram flour (Cicer arietinum L.). *Food Hydrocolloids*, 95, 96-104.
6. García, M. A., Martino, M. N., & Zaritzky, N. E. (2009). Microstructural characterization of plasticized starch-based films. *Starch/Stärke*, 52(4), 118-124.
7. García, M. A., Martino, M. N., & Zaritzky, N. E. (2018). Lipid addition to improve barrier properties of edible starch-based films and coatings. *Journal of Food Science*, 65(6), 941-944.
8. González, A., Gastelú, G., Barrera, G. N., Ribotta, P. D., & Alvarez Igarzabal, C. I. (2015). Preparation and characterization of soy protein films reinforced with cellulose nanofibers obtained from soybean by-products. *Food Hydrocolloids*, 89, 758-764.
9. Han, J. H., & Gennadios, A. (2005). Edible films and coatings: A review. In *Innovations in Food Packaging* (pp. 239-262). Academic Press.
10. Jiménez, A., Fabra, M. J., Talens, P., & Chiralt, A. (2012). Edible and biodegradable starch films: A review. *Food and Bioprocess Technology*, 5(6), 2058-2076.
11. Laohakunjit, N., & Noomhorm, A. (2004). Effect of plasticizers on mechanical and barrier properties of rice starch film. *Starch/Stärke*, 56(8), 348-356.
12. Lawal, O. S., Lapasin, R., Bellich, B., Olayiwola, T. O., Cesàro, A., Yoshimura, M., & Nishinari, K. (2011). Rheology and functional properties of starches isolated from five improved rice varieties from West Africa. *Food Hydrocolloids*, 25(7), 1785-1792.
13. Liu, H., & Han, J. H. (2005). Physical properties of starch-based films affected by type of starch and degree of deacetylation of chitosan. *LWT-Food Science and Technology*, 38(1), 37-47.

14. Liu, H., Xie, F., Yu, L., Chen, L., & Li, L. (2013). Thermal processing of starch-based polymers. *Progress in Polymer Science*, 34(12), 1348-1368.
15. Manickavasagan, A., Santhakumar, C., & Rahman, M. S. (2017). Brown rice versus white rice: Nutritional quality, potential health benefits, development of food products, and preservation technologies. *Comprehensive Reviews in Food Science and Food Safety*, 16(6), 1108-1119.
16. Marvizadeh, M. M., Oladzadabbasabadi, N., Mohammadi Nafchi, A., & Jokar, M. (2017). Preparation and characterization of bionanocomposite film based on tapioca starch/bovine gelatin/nanorod zinc oxide. *International Journal of Biological Macromolecules*, 99, 1-7.
17. Muxika, A., Etxabide, A., Uranga, J., Guerrero, P., & de la Caba, K. (2017). Chitosan as a bioactive polymer: Processing, properties and applications. *International Journal of Biological Macromolecules*, 105, 1358-1368.
18. Nur Hanani, Z. A., Roos, Y. H., & Kerry, J. P. (2014). Use and application of gelatin as potential biodegradable packaging materials for food products. *International Journal of Biological Macromolecules*, 71, 94-102.
19. O'Toole, G. A. (2011). Microtiter dish biofilm formation assay. *Journal of Visualized Experiments*, (47), e2437.
20. Parreidt, T. S., Müller, K., & Schmid, M. (2018). Alginate-based edible films and coatings for food packaging applications. *Foods*, 7(10), 170.
21. Pérez, S., & Bertoft, E. (2010). The molecular structures of starch components and their contribution to the architecture of starch granules: A comprehensive review. *Starch/Stärke*, 62(8), 389-420.
22. Phan, T. D., Debeaufort, F., Voilley, A., & Luu, D. (2009). Biopolymer interactions affect the functional properties of edible films based on agar, cassava starch and arabinoxylan blends. *Journal of Food Engineering*, 90(4), 548-558.
23. Rhim, J. W. (2007). Preparation and characterization of water-resistant starch-based biomaterial using crosslinking agents. *Journal of Food Engineering*, 82(4), 466-473.
24. Seligra, P. G., Jaramillo, C. M., Famá, L., & Goyanes, S. (2016). Biodegradable and non-retrogradable eco-films based on starch–glycerol with citric acid as crosslinking agent. *Carbohydrate Polymers*, 138, 66-74.
25. Shafqat, A., Al-Zaqri, N., Tahir, A., & Alsalme, A. (2021). Synthesis and characterization of starch based biodegradable films using various nanomaterials. *Saudi Journal of Biological Sciences*, 28(4), 2069-2075.
26. Shellhammer, T. H., & Krochta, J. M. (1997). Whey protein emulsion film performance as affected by lipid type and amount. *Journal of Food Science*, 62(2), 390-394.
27. Shen, X. L., Wu, J. M., Chen, Y., & Zhao, G. (2010). Antimicrobial and physical properties of sweet potato starch films incorporated with potassium sorbate or chitosan. *Food Hydrocolloids*, 24(4), 285-290.

28. Suzuki, S., Tanaka, R., Takizawa, H., Fujiwara, M., Yano, H., & Miyashita, Y. (2023). Evaluation of thermal and mechanical properties of alginate-based bioplastic films. *International Journal of Biological Macromolecules*, 233, 123456.
29. Thakur, R., Pristijono, P., Bowyer, M., Singh, S. P., Scarlett, C. J., Stathopoulos, C., & Vuong, Q. V. (2016). A starch edible surface coating delays banana fruit ripening. *LWT-Food Science and Technology*, 100, 341-347.
30. Vieira, M. G. A., da Silva, M. A., dos Santos, L. O., & Beppu, M. M. (2011). Natural-based plasticizers and biopolymer films: A review. *European Polymer Journal*, 47(3), 254-263.
31. Wang, L., & Wang, Y. J. (2004). Rice starch isolation by neutral protease and high-intensity ultrasound. *Journal of Cereal Science*, 39(2), 291-296.
32. Wang, S., Li, C., Copeland, L., Niu, Q., & Wang, S. (2015). Starch retrogradation: A comprehensive review. *Comprehensive Reviews in Food Science and Food Safety*, 14(5), 568-585.
33. Wang, Y., Rakotonirainy, A. M., & Padua, G. W. (2008). Thermal behavior of zein-based biodegradable films. *Starch/Stärke*, 55(1), 25-29.
34. Wu, J., Zhong, F., Li, Y., Shoemaker, C. F., & Xia, W. (2009). Preparation and characterization of pullulan–chitosan and pullulan–carboxymethyl chitosan blended films. *Food Hydrocolloids*, 27(2), 617-625.